



Defect tolerance under level D loading

Hooton D.G.

AEA Technology, United Kingdom

ABSTRACT

The paper presents the results of a study into the sensitivity of a representative reactor structure to the presence of defects. In particular, results of a pressure test to failure of a 40% scale model of an intermediate heat exchanger (IHX) and associated inelastic finite element analysis are presented. Design code assessments in accordance with the Level D criteria of the ASME and RCC-M codes indicate that design limits are not infringed by realistic defects that may occur in practice, and that allowable pressure is best indicated by collapse load analysis.

INTRODUCTION

A large displacement inelastic FE analysis of an IHX, subjected to a postulated sodium-water reaction transient, [1,2] highlighted the need for guidance in interpreting the Level D criteria of ASME III [3], and proposed replacement of the plastic instability criterion by strain limits. To corroborate this interpretation of Level D criteria, scale models incorporating the salient lower tubeplate and outer shell features of the IHX, including manufacturing defects, were pressurised to failure, [2]. Pressures at failure were then compared with those determined from Level D criteria with stress and strain values determined by large displacement inelastic FE analysis. In this paper results of these analyses are reviewed and further compared with code limits of the collapse load analysis of Appendix II of ASME III [3] and Appendix ZF of RCC-M [4]. Postulated defects in the axial seam weld of the IHX are also analysed using the R6 method [5], and results presented as tolerable defect sizes for class 1 and class 2 vessels, on the basis code allowable elastic stress limits.

MODEL TESTS

Two hydraulic burst tests were performed on 40% scale models incorporating the outer shell and lower tube plate features of an IHX and manufactured from 316 stainless steel, Figure 1. The outer shell was manufactured from 6.35 mm thick sheet steel which was rolled and then seam welded, without post-weld heat treatment. The 20 mm thick tubeplate contained 298 x 19 mm diameter holes on a triangular pitch, with the same ligament efficiency as a full size IHX. The weld preparation and procedures for the partial penetration connecting weld

between the tubeplate and outer shell, detail shown Figure 2, were similar to that on a full size IHX.

Strain gauges were positioned along the outer surfaces of the outer shell and tubeplate and displacements were measured at the centre of the tubeplate and the at the shell mid-height positions, Figure 3. Readings of pressure were recorded during the tests.

The pressures at failure for the two vessels were 7.8 MPa and 8.7 MPa, although it should be noted that the former had to be depressurised and reloaded due to leakage problems during the test. In both cases, failure occurred across the outer shell adjacent to the crevice of the tubeplate partial penetration weld and then propagated rapidly around the circumference.

Post-test examination of the first vessel revealed that failure probably initiated due to lack of fusion in the circumferential shell/tubeplate weld, in line with the axial seam weld. Metallographic examination indicated defects up to 3mm deep (approximately 50% of wall thickness) in the through-thickness direction of the shell. For the second vessel, failure initiated at a position slightly off-set from the axial weld, although again evidence of lack of fusion (but to a lesser extent) was present. There was good agreement between trends of the strain response and vessel deformations of the two tests, the tubeplate doming downwards and the outer shell displacing outwards due to the internal pressure loading. These distortions concentrated considerable bending strains in the vicinity of the lower tubeplate to outer shell connection, and together with the lack of fusion in the circumferential weld, were probably the cause of failure of both vessels.

CODE ASSESSMENT

Results of the elastic and non-linear large displacement FE analyses [2] were assessed using the rules of ASME III [3] Appendix F (F-1341), which allow acceptability to be demonstrated using any one of the following methods: (a) elastic analysis, (b) plastic analysis, (c) collapse load analysis, (d) plastic instability analysis, (e) interaction method. Of these methods only (a) and (b) were applied directly, (c) was omitted, (e) is not relevant, and (d) was replaced by strain limits. A load-controlled strain limit was taken at 35%, the true strain in a test specimen at the UTS, and a strain-controlled limit was taken at 50%, the true strain at test specimen failure.

The replacement of the plastic instability criterion by strain limits was based on the understanding that large displacement FE analysis does not reproduce the necking associated with load controlled instability, and therefore, plastic instability determined from an asymptote to a load-deflection curve could lead to incorrect values of failure pressure. Hence, instability was defined by a strain limit corresponding to the strain at UTS in materials test specimens.

In consideration of a strain controlled limit, it was noted that at structural discontinuities, code methods make no reference to appropriate criteria for displacement controlled strains, since it is assumed that these regions will follow the displacement of adjacent load controlled members. However, strains in discontinuity regions may reach ductility limits before the plastic instability load is achieved in adjacent load controlled

members. Hence, limiting strain was defined as that corresponding to the strain at failure in materials test specimens.

Code assessments were made at three critical locations: (1) junction of cylindrical shell and tube plate, (2) tube plate (junction at inner hub), (3) mid-point of cylindrical shell. Results for allowable pressure are summarised in Table 1.

| Location | Method of Assessment | | |
|---------------|----------------------|---------------------|------------------|
| | a) Elastic analysis | b) Plastic analysis | d) Strain limits |
| 1 | 0.75 | 1.50 | (3.62) |
| 2 | 0.86 | 1.30 | 6.02 |
| 3 | 8.89 | >10 | >10 |
| Minimum value | 0.75 | 1.30 | 6.02 |

TABLE 1 - Allowable pressure (MPa)

Method (d) was not considered applicable to location (1), as the strain at this point is not indicative of the load carrying capacity of the structure. (This point was, however, the point of failure). Hence, the allowable pressure was taken to be 6.02 MPa, the highest minimum value of pressure given by any method. This compared with test failure pressures [3] of 7.80 MPa and 8.70 MPa.

However, the interpretation of stress classifications [2], for methods (a) and (b), at locations (1) and (2), (i.e. all stresses classified as primary, including peak stresses, which by definition do not contribute to failure), could be considered unduly conservative. Also, the load controlled strain limit (method d) at location 2 would not appear to be a good measure of failure, as experimental values of strain and displacement in the tubeplate varied linearly with pressure right up to failure.

For both tests, failure occurred at the welded junction, which was not modelled in the FE analysis. Post-test examination revealed that failure initiated from lack of fusion defects. A better comparison of analysis and test results might therefore be obtained using method (c), collapse load analysis, which will not be influenced by the presence of defects, to the same extent as instability (or strain limit) analysis.

Collapse load analysis

Collapse loads are determined from load/strain (or displacement) diagrams, e.g. Figure 3, using the method of Appendix II [3]. This method replaces former ASME III methods, one based on equal elastic and plastic distortions, and another based on twice the angle the linear part of the load-deflection curve makes with the load axis.

Experimental results for load vs. strain/displacement, e.g. Figure 3, and FE results [2] used for the calculation of collapse load are given in Table 2, and resultant values for

experimental and analytical collapse pressures are given in Table 3. (Note: These are ASME values, a factor of 0.9 is applied to these values in RCC-M).

It should also be noted that allowable pressure determined by collapse load analysis is dependent on strain history. Since Test 1 was conducted in two phases, with stress levels in the cylinder well in excess of yield during the first phase, these results are not considered strictly valid for collapse load analysis.

| | | | | | | | |
|------------|--------|--------|--------|--------|--------|--------|--------|
| Press. MPa | 1.42 | 2.45 | 3.94 | 5.95 | 8.02 | 9.45 | 10.00 |
| Disp.mm | 0.0678 | 0.1179 | 0.1899 | 0.4864 | 1.7400 | 3.9230 | 5.4330 |
| Strain % | 0.024 | 0.041 | 0.066 | 0.231 | 1.064 | 2.542 | 3.564 |

TABLE 2 - FE results for radial displacement and hoop strain at cylinder mid-point

| | Gauge | | | | | | Disp.at 6 |
|--------|-------|------|------|------|------|------|-----------|
| | 1 | 2 | 6 | 7 | 8 | 9 | |
| Test 1 | 7.48 | 7.58 | 6.69 | 7.49 | - | - | - |
| Test 2 | - | - | 5.07 | - | 3.03 | 3.55 | 6.14 |
| F.E. | - | - | 5.70 | - | - | - | 6.20 |

TABLE 3 - Collapse Pressure (MPa)

Both Appendices II [3] and ZII [4] state that for collapse load calculations, care should be taken to ensure that strains are actually indicative of the load carrying capacity of the structure, and displacements are indicative of the tendency of the structure to actually collapse. On this basis gauges 8 and 9 can be ignored. (This is supported by tubeplate displacement measurements which indicated enhanced load carrying capacity of the tube plate when plastic hinges are formed at the locations of gauges 8 and 9, Figure 2). Hence, collapse pressure is best indicated by gauge 6, where there is reasonable agreement between both strain gauge and displacement results with a minimum allowable pressure for test 2 of 5.07 Mpa, Table 2.

It is also interesting to note good agreement between the collapse pressure determined using the experimental values of displacement at gauge 6 (6.14 MPa) and that determined using FE results (6.20 MPa), (note that FE results for strain are rather less than for displacement due small bending strains at the surface). Further, instability pressure determined from the asymptote to the experimental load displacement curve at point 6 is in agreement with the experimental value of pressure at failure (8.70 MPa), and an allowable pressure based plastic instability analysis, ($P=0.7 \times P_1=6.09$ MPa), is in agreement with collapse load analysis. The displacement at point 6, the mid-point of the cylindrical shell, therefore provides a good indication of the load carrying capacity of the vessel, with an allowable pressure, determined analytically, of 6.20 MPa.

DEFECT ASSESSMENT

The model test assessment indicates that small defects present in the crevice region of the weld had little effect on the failure of the vessel. i.e. there was reasonable agreement between assessments based on experimental results and theoretical results that ignored the presence of small defects. In this section, therefore, attention is focused on postulated axial defects in the mid-section of the axial seam weld of the cylindrical part of the vessel, rather than at the vessel supports. Results are presented as tolerable defect sizes for class 1 and class 2 vessels, on the basis of elastic allowable stress limits.

Analysis of cylindrical section of Model test

Taking the geometry and material properties of the model test:

cylinder internal radius=281.94 mm, thickness=6.35 mm
 $\sigma_y = 251$ MPa, $\sigma_U = 646$ MPa (parent material)
 fracture toughness, $K_{0.2} = 3800$ Nmm^{-3/2} (weld metal at RT)

crack driving force curves, K_F , using the methods of R6 [5] may be described by the equation

$$K_F = K_I \left[\left(1 - 0.14L_r^2 \right) \left\{ 0.3 + 0.7 \exp(-0.65L_r^6) \right\} \right]^{-1}$$

where K_I is the linear elastic stress intensity factor, and $L_r = P / P_L(a, \sigma_y)$ where a is crack size, P represents the magnitude of the applied load and P_L is the corresponding magnitude at plastic collapse for yield stress σ_y , with a cut-off defined by

$$L_r^{\max} = \frac{\bar{\sigma}}{\sigma_y} \quad \text{where} \quad \bar{\sigma} = \frac{\sigma_y + \sigma_u}{2}$$

Comparison of crack driving force curves, as functions of crack aspect ratio and depth, with materials fracture resistance then allows limiting crack sizes to be determined for varying values of applied load, and for various levels of fracture toughness based on varying degrees of stable tearing, as illustrated in Figure 5. Hence, limiting crack sizes may be determined for code allowable pressures evaluated using code limits [3,4]. Results of Figure 5 show a minimum value of relative depth of 12.5% is indicated for a defect aspect ratio (a/c =crack depth/ semi-length) of 0.1 and 35% for a semi-circular defect $a/c=1$.

Comparisons of crack driving force curves plotted against crack depth with the materials fracture toughness resistance curve [6], for $a/c=0.1$, has shown that, for crack depths of up to half the section thickness, crack instability occurred at initiation values of toughness, due to the steep gradient of the driving force curves. Hence, for these cases no advantage may be taken of increased toughness with crack growth.

For $a/c=1$, similar comparisons, have shown significant stable tearing before failure at plastic collapse, based on a flow stress of $(S_y + S_u) / 2$, which is approximately $0.7S_u$.

It may be noted that on Figure 5 the allowable pressure for a defect free structure, ($a/t=0$), using the R6 method is based on a flow stress which is the mean of the yield and ultimate stress, 448.5 MPa, (which is approximately $0.7S_{u}$, 452 MPa), whereas, P_c is based on a flow stress of $2.3S_m$ (the lesser of $2.3S_m$ and $0.7S_{u}$, 384 MPa), with a factor of 0.9 applied. Therefore, the calculated tolerable defect sizes, indicated on this diagram, arise from code margin on material properties and applied safety factors.

Hence, results from this comparatively simple example indicate the complexity of defect tolerance under Level D loading. It is not possible to draw general conclusions from these results, but the need to be aware of differences in material tensile properties used in defect assessment procedures and design code criteria is emphasised.

CONCLUSIONS

Design code assessments of a 40% scale model of an austenitic intermediate heat exchanger have indicated, by comparison with experiment, that allowable pressure loading, determined using Level D criteria, is best estimated by collapse load analysis using results from inelastic large displacement finite element analysis. Whereas, stress limits at the point in the component where displacements are indicative of the load carrying capacity, i.e. the mid-point on the cylinder axis; the point used in the collapse load analysis, may not provide for conservative assessments. This situation is contrary to the statement of ASME [3] Appendix F (F-1341) and RCC-M [4] Appendix ZF (ZF-1322.2) that acceptability of a component may be demonstrated using any one of the methods therein.

Comparison of experimental and finite element results also indicates that the collapse method gives sufficient margin for small lack of fusion defects, at the cylinder/shell weld, present in the test model but not included in the finite element analysis.

The assessment of defects in a cylindrical vessel and their influence on allowable loading has shown that the combinations of material properties and defect sizes, even for this simple case, do not allow for the formulation of general rules defining acceptable defect sizes under level D loading. The effect of defects should, therefore, be studied on an individual case basis.

ACKNOWLEDGEMENT

The work described in this paper was carried out under CEC Contract ETNU-92-0074. The paper is published with permission of AEA Technology plc.

REFERENCES

1. Smith N G and F Rohdenburg. Elastic and inelastic analyses to examine margins on Level D criteria. *SMiRT 11 Transactions* Vol. E, pp 113-118, (August 1991).

2. Smith N G. Second Milestone Report on Margins on Level D criteria. AGT9B-SG1 Report, (March 1992).

3. American Society of Mechanical Engineers Boiler and Pressure Vessel Code Section III. Rules for the Construction of Nuclear Power Plant Components. (1992).

4. Design and Construction Rules for Mechanical Components of PWR Nuclear Islands (RCC-M), AFCEN, Paris. (1988).

5. Milne, I, R A Ainsworth, A R Dowling and AT Stewart. Assessment of the integrity of structures containing defects. *Int. J Pres Ves & Piping* 32, 3-104 (1988).

6. Hooton D G, S K Bate, D Moulin, G Clement and C Gregoire. Defect tolerance under level D loading. CEC Contract ETNU-92-0074. (1994).

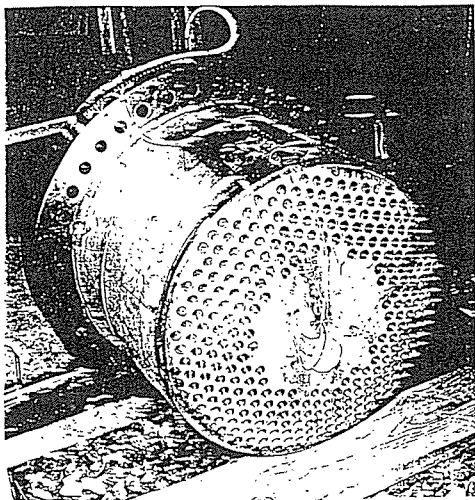


FIG. 1- Test Vessel General View

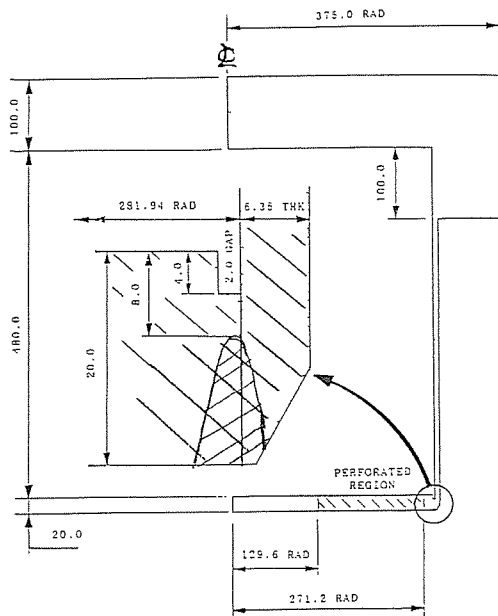


FIG. 2- Geometry of Test Vessel

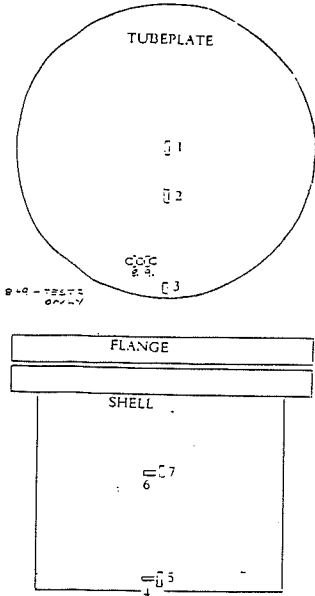


FIG.3- Position of Strain Gauges

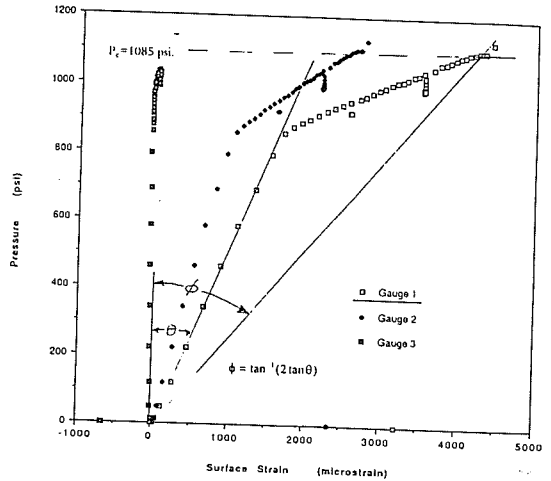


FIG. 4- Determination of Collapse Pressure Point 1 (Test 1)

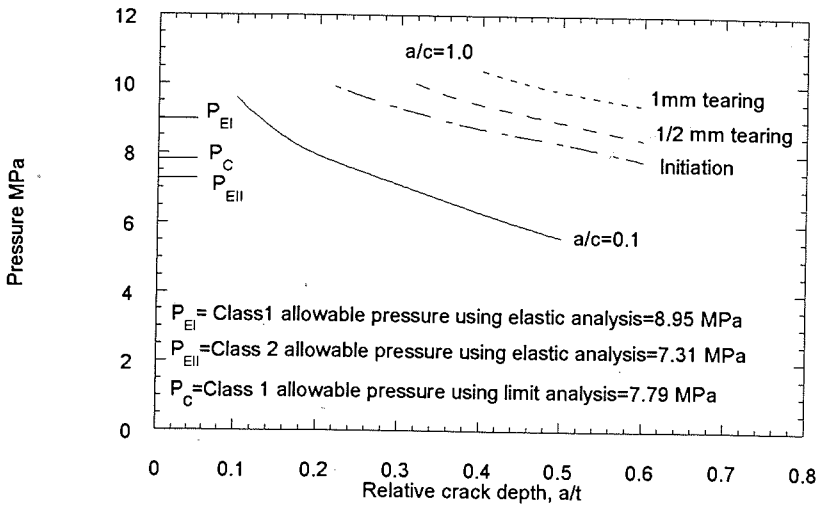


FIGURE 5- Tolerable defect sizes under Level D loading